Wall heat flux influence on the thermodynamic optimisation of irreversibilities of a circulating fluidised bed combustor

J Baloyi[1, 2], T Bello-Ochende[3, *] and JP Meyer[1]
Author for correspondence
[1]Department of Mechanical and Aeronautical Engineering, University of Pretoria, Private Bag X20, Hatfield, Pretoria, 0028, South Africa
[2]Modelling and Digital Science, Council for Scientific and Industrial Research, P.O. Box 395, Pretoria, 0001, South Africa
[3]Department of Mechanical Engineering, University of Cape Town, Private Bag X3, Rondebosch, 7701, South Africa
Email: tunde.bello-ochende@uct.ac.za

Abstract
In the study the comparison of irreversibilities was done when the wall condition of the combustor was changed from adiabatic to negative heat flux, for incoming air temperature of 400 K. The reactant mixture of solid pitch pine wood fuel and air was varied from a rich to a lean mixture. A non-adiabatic non-premixed combustion model of a numerical code (ANSYS FLUENT 16.2) was used to simulate the combustion process where the solid fuel was modelled by using the ultimate analysis data. The irreversibilities generated were arrived at by computing the entropy generation rates due to the combustion and frictional pressure drop processes. For the combustor where the wall condition was changed from adiabatic to negative heat flux (that is heat leaving the system) the minimum irreversibilities generated changed from occurring at an equivalence ratio of 1.67 for an adiabatic wall condition to 1.34 for a negative heat flux wall condition. It was also found that the penalty paid when deviating from the equivalence ratio of 1 at which minimum irreversibilities are generated is drastically increased due to less heat in the combustor resulting more unburnt fuel exiting the combustor.

Introduction

The focus of the world is the reduction of greenhouse gases like carbon dioxide. Since most of the carbon dioxide emitted into the atmosphere is from fossil fuel combustion, alternative energy source were developed and others are currently under study to see if they can make good alternatives. One of these alternative sources of energy is the combustion of wood in place of coal. However wood has lower calorific heat rates than coal, so the investigation of better conditions under which to run combustion chambers burning wood is paramount if wood is to make a good alternative source of energy. Norton and Vlachos [1] found two modes of flame blowout, one due to thick wall thermal conductivities and another due to low flow velocities when they numerically studied the effects of wall thickness and flow velocities on the combustion characteristics and flame stability in a premixed methane/air mixture micro-burner. Zhang et al. [2] used a heat recovery steam generator (HRSG) to enhance the energy efficiency of a polygeneration plant. By optimising the HRSG using the mixed-integer nonlinear programming approach they found that optimum depended on the HRSG type and model specification. Kohl et al. [3] analysed the exergetic and economic performance of three biomass upgrading processes where three fuels namely wood pellets, torrefied wood pellets and a mixture of pyrolysis char and oil, were put through a pyrolysis process. They found that most of the exergy destruction occurred in the combustion equipment, but the exegetic efficiencies for the three fuels were improved by 22%, 26% and 31% for the mixture of pyrolysis char and oil, torrefied wood pellets and wood pellets respectively. But the economic performance was best for the mixture of pyrolysis char and oil. Li et al. [4] analysed the exergy performance of three coals to synthetic natural gas and power cogeneration systems with or without carbon dioxide capture. They found the system with carbon dioxide capture had more exergy loss than the system without, and the cogeneration systems had lower exergy input requirements when compared to single product systems. Safari, Reza and Sheikhi [5] used large eddy simulation that incorporated the entropy transport equation to analyse entropy generation in a turbulent non-premixed flame. They found chemical reaction and heat conduction were the main sources of irreversiblities in the flame.

Nguyen et al. [6] conducted a thermodynamic evaluation of oil and gas platforms to find system efficiencies of over the life cycle of the platforms. They found around 50% of the inefficiencies were

due to chemical exergy inefficiencies, 20% due to thermal exergy inefficiencies and 15% due to mechanical exergy efficiencies. Hagi et al. [7] performed an exergy analysis on oxy-fire pulverised coal power plants in the pursuit of minimising the exergy losses while taking into account the technological and operational constraints. The plants looked at were the conventional cold flue gas recycle scheme and three alternative flue gas recirculation schemes. They found the alternative scheme with recirculation of the flue gas before the regenerative heat with advanced air separation unit and a double column compression and purification unit had the highest net plant efficiency. Li et al. [8] developed a theoretical framework for the exergy analysis of a biomass boiler by conducting sensitivity studies of several design parameters like excess air, steam parameters and biomass moisture. They found that most of the exergy destruction occurred in the combustion process, followed by water walls and radiation superheater, and then the low temperature superheater. The technique of analysing and minimising the entropy generation rate of a process was demonstrated with good effect in studies by [9-12]. In furtherance of the work done in Baloyi, Bello-Ochende and Meyer [9] and Baloyi, Bello-Ochende and Meyer [13], in this study the effect of changing the wall condition on a circulating fluidised bed combustor from adiabatic to negative heat flux (that is heat leaving the system) on the equivalence ratio value at which minimum irreversibilities are generated was also investigated. Because the sum of the molar fractions of the combustion products species must add up to one, when the molar fraction of one of the species increases, the molar fractions of the other species will either increase or decrease to result in a sum of one. With this fact in mind the link between the change in optimum equivalence ratio and the balance between the molar fractions of the combustion products species was also investigated.

Nomenclature

Abbreviation

CFD	Computational Fluid Dynamics

Symbol

A	Cross-sectional area [m^2]
AF	Air-fuel mass ratio
$\bar{c}$	Molar specific heat [kJ/kmol.K]
c	Specific heat [kJ/kg.K]
c_p	Specific heat at constant pressure [J/kg.K]
C	Atomic carbon
CO	Carbon monoxide
CO_2	Carbon dioxide
D	Combustor diameter [m]
ER	Equivalence ratio
g	Gravitational acceleration magnitude [m/s^2]
G	Mixture mass flux [kg/s/m^2]
$\bar{h}$	Specific enthalpy [k/kmol]
$\bar{h}^0$	Enthalpy of formation [J/kmol]
H	Atomic hydrogen; Height [mm]; total enthalpy [J]
H_2	Molecular hydrogen
H_2O	Water vapour
$\dot{I}$	Irreversibility [W]
L	Length [m]
$\dot{m}$	Mass flow rate [kg/s]
M	Molecular weight [kg/kmol]
n	Stoichiometric coefficient
N	Atomic nitrogen; Entropy generation number
N_2	Molecular nitrogen
O	Atomic oxygen
O_2	Molecular oxygen
P	Pressure [Pa]
q''	Wall heat flux [W/m^2]
$\bar{R}$	Universal gas constant [J/kmol.K]
$\bar{s}$	Specific entropy [J/kmol.K]
$\bar{s}^\circ$	Absolute entropy [J/kmol.K]
$\dot{S}_{gen}$	Entropy generation rate [W/K]
T	Temperature [K]
x	Molar fraction

Greek symbol

ρ	Density [kg/m^3]
ε	Void fraction; turbulent dissipation rate
μ	Molecular viscosity [Pa.s]

Subscript

0	Superficial
Air	Air
$char$	Char
CO	Carbon monoxide
CO_2	Carbon dioxide
f	Fuel
g	Gas
$gen,\min$	Minimum entropy generation rate
$gen(h)$	Entropy generation rate due to heat
$gen(p)$	Entropy generation rate due to frictional pressure drop
H_2	Molecular hydrogen
H_2O	Water vapour
$h-t$	Heat transfer
i	Counting index
l	Maximum number of products
m	Maximum number of reactants; mixture
mf	Minimum fluidisation
N_2	Molecular nitrogen
O_2	Molecular oxygen
p	Product species
r	Reactant species
ref	Environment reference
s	Solid species
sd	Dense zone solid species
se	Exit zone solid species
t	Total of solid and gas
th	Theoretical amount of air ratio

Method

Exergy analysis

The irreversibility generation rate that results from the combustion-heat transfer and frictional pressure drop processes taking place in an adiabatic combustor is as given by equation (1) [15].

$$\dot{I} = \frac{\dot{m}_f}{M_f}\left(\sum_{i=1}^{m} n_{ri}\left(\bar{h} - T_{ref}\bar{s}\right)_{ri} - \sum_{i=1}^{l} n_{pi}\left(\bar{h} - T_{ref}\bar{s}\right)_{pi}\right) \quad \textbf{(1)}$$

Since the sums of the enthalpy terms cancel out and entropy terms of the combustion products are unknowns for a rich mixture in equation (1), the irreversibility generation rate can also be defined by equation (2)

$$\dot{I} = T_{ref}\dot{S}_{gen} \quad \textbf{(2)}$$

where $\dot{S}_{gen}$ is the entropy generation rate.

The study focused on comparing the combustor with an adiabatic wall condition and incoming air temperature of 400 K (case 1) to a combustor with a negative heat flux wall condition (case 2), which also has an incoming air temperature of 400 K.

The chemical formula of the solid fuel as computed in [13] is given by $C_{4.9}H_{7.2}O_2$, the lower heating value of the fuel from [13] was given as 16091.2 kJ/kg and the molecular weight of the fuel was calculated as 98 kg/kmol. The specific heat at constant pressure was also given as 1.680 kJ/kg.K. For case 2 a negative wall heat flux of 7 500 W/m^2 was applied over the wall of the combustor cases with AF varying from 4.5 to 10 (equivalence ratio from 1.782 to 0.802 respectively) for an air inlet temperature of 400 K, as shown in Figure 1. The selected range of AF corresponds to mixture varying from a rich mixture to a lean mixture. The 7 500 W/m^2 heat flux resulted in a heat rate of energy extracted through the wall of 48.5 kW$_{th}$. This corresponds to about 20% of the total thermal heat rate of 241 kW$_{th}$ generated in the combustor for a fuel mass flow rate of 0.015 kg/s.

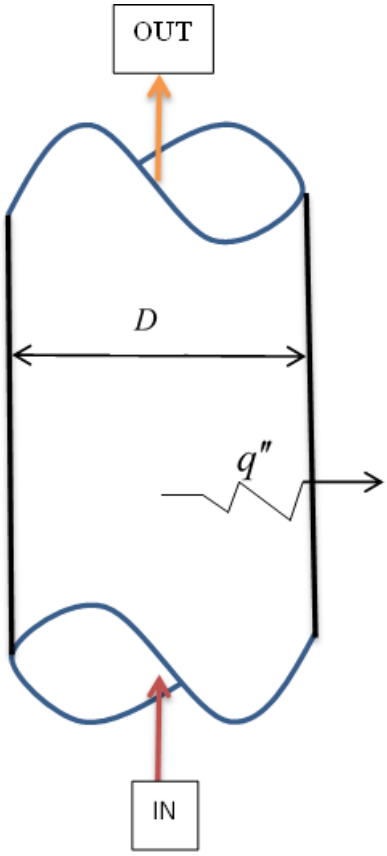

Figure 1 Sketch of a combustor section with negative heat flux wall condition and zero wall thickness

The analysis of the entropy generation rate is the same as that of [9] except that there is an additional term due to heat transfer [17] through the wall of the combustor, and this term is as expressed in equation (3).

$$\dot{S}_{gen(h-t)} = -\frac{2\pi LDq''}{T_m + \Delta T} \quad \textbf{(3)}$$

Where L is the length of the combustor, D is the diameter of the combustor, q'' is the wall heat flux and ΔT is the change in temperature across the length of the combustor. The only term that is unknown in equation (3) is ΔT which can be described by equation (4).

$$\Delta T = \frac{q''}{c_p GSt} \quad \textbf{(4)}$$

Where $G = \dot{m}_f\left(AF + 1\right)/A$ is the mixture mass flux and $St = Nu/\mathrm{Re}_D\,\mathrm{Pr}$ is the Stanton number. The Prandtl number Pr is assumed to be 0.69 [19] for the gas species mixture involved in the combustion process and Re_D is the Reynolds number based on

the combustor diameter. The Nusselt number [17] is given by equation (5), assuming fully turbulent internal flow.

$$Nu = 0.023\,\mathrm{Re}_D^{\,0.8}\,\mathrm{Pr}^{0.4} \qquad \textbf{(5)}$$

Substituting equation (5) into equation (4) and taking all the above into consideration, equation (4) becomes:

$$\Delta T = \frac{\pi D^2 q''}{0.1148 c_p \dot{m}_f (AF+1)\mathrm{Re}_D^{-0.2}} \qquad \textbf{(6)}$$

Substituting equation (6) into equation (3) results in:

$$\dot{S}_{gen(h-t)} = -\frac{0.2296\pi L D c_p \dot{m}_f (AF+1) q'' \mathrm{Re}_D^{\,-0.2}}{0.1148 c_p \dot{m}_f (AF+1) T_m \mathrm{Re}_D^{\,-0.2} + \pi D^2 q''} \qquad \textbf{(7)}$$

When equation (7) is added to the equation derived in [9], what results is an equation that describes the entropy generation rate due combustion and heat transfer through a wall for the combustor with a heat flux wall condition, as expressed by equation (8).

$$\dot{S}_{gen} = \frac{\dot{m}_f}{M_f}\left(\begin{array}{l}\sum_{j=1}^{l} n_{pj}\left(\bar{s}^\circ - \bar{R}\ln(x)\right)_{Pj} - \sum_{j=1}^{m} n_{rj}\left(\bar{s}^\circ - \bar{R}\ln(x)\right)_{rj} \\ + \frac{\rho_{char}}{\rho_g} n_{char} c_{char} M_{char} \ln\left(T_{char}/298\right) \\ - \frac{\rho_f}{\rho_g} n_f c_f M_f \ln\left(T_f/298\right)\end{array}\right) - \frac{0.2296\pi L D c_p \dot{m}_f (AF+1) q'' \mathrm{Re}_D^{\,-0.2}}{0.1148 c_p \dot{m}_f (AF+1) T_m \mathrm{Re}_D^{\,-0.2} + \pi D^2 q''} \qquad \textbf{(8)}$$

where the Reynolds number is as expressed by equation (9).

$$\mathrm{Re}_D = \frac{4\dot{m}_f (AF+1)}{\pi \mu_m D} \qquad \textbf{(9)}$$

where μ_m is the mixture dynamic viscosity.

The entropy generation number, N_s [9] which is the quotient of the entropy generation rate at any Reynolds number and the minimum entropy generation rate, was used to analyse the penalty paid by running the combustor at a Reynolds number other than the optimum and is as given by equation (10).

$$N_s = \frac{\dot{S}_{gen}}{\dot{S}_{gen,\min}} \qquad \textbf{(10)}$$

The relative generation rate, N_R [9], which is the quotient of the entropy generation rate at any equivalence ratio, and the entropy generation rate when combustion occurred with theoretical air ratio, is as expressed by equation (11).

$$N_R = \frac{\dot{S}_{gen}}{\dot{S}_{gen,th}} \qquad \textbf{(11)}$$

The equivalence ratio is related to the Air-Fuel mass ratio as: $ER = AF / AF_{th}$.

Numerical model

The combustor produced 241 kW_{th} when complete combustion of pitch pine wood occurs with theoretical amount of air. The combustor had a diameter of 300 mm and a height of 7 000 mm as illustrated in Figure 2.

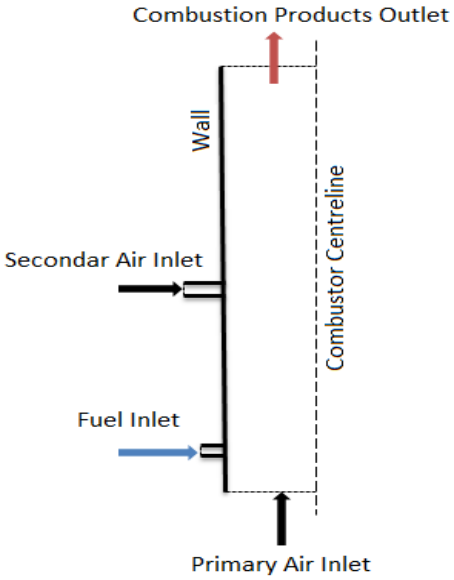

Figure 2 Schematic of the combustor showing boundary placements

The mass flow rate of the incoming solid fuel was fixed at a value of 0.015 kg/s so as to have a common maximum heat generation rate of 241 kW_{th} since the lower heating value is fixed and unique for any particular fuel. ANSYS FLUENT 16.2 [18] was used to simulate the combustion process inside the combustor. The combustion process was modelled using the non-premixed combustion model, because the solid fuel is only specified in the form of ultimate analysis data [19], and the combustion model gives an option of specifying the fuel as an empirical stream. The inlet diffusion option was selected.

The use of the chosen combustion model required the use of a turbulent model, because the combustion model is a mixture model. To this end the $k-\varepsilon$ turbulent model with enhanced wall function option was chosen for all simulations. The P1 model included in the ANSYS FLUENT 16.2 code [18] was used to model radiation.

The combustor had four mass flow inlets for the solid fuel, each with equal mass flow rate of 0.00375 kg/s. The inlet temperature of the fuel at each inlet was set at 600 K. The temperature value was selected to be the same as the devolatilisation temperature of pitch pine [19]. The oxidising air was split into the primary and secondary air, each making up half of the total air used in the oxidation of the fuel. The reason for splitting the oxidising air was to enable the modelling of incomplete combustion to take place. The primary air entered the combustor at the base with a single fixed mass inlet, with half of the total air mass flow rate. The secondary air four fixed mass inlets were situated a quarter of the height up the combustor, each having an eighth of the total air mass flow rate. The inlet temperature at all eight air inlets was set at 400 K. The wall boundary condition of the combustor was a negative heat flux of 7 500 W/m^2 or adiabatic depending on the case. The data that was extracted from the simulations were the temperature at the pressure outlet boundary and the combustion products molar fractions.

Results and discussion

The entropy generation rate and irreversibilities of case 1 and case 2 were compared in order to observe the effect of a wall heat flux, and the results are presented in Figure 3. It can be seen from Figure 3 that the application of a negative heat flux resulted in a drastic increase in the entropy generation rate. By changing the wall condition from adiabatic (case 1) to negative heat flux (case 2) the ER at which the minimum entropy generation rate and irreversibilities occurred changed from 1.67 to 1.34. This can be clearly seen in Figure 4 where a plot, with a bound range in the AF axis, of the entropy generation rate is plotted around the AF value where the minima occurred.

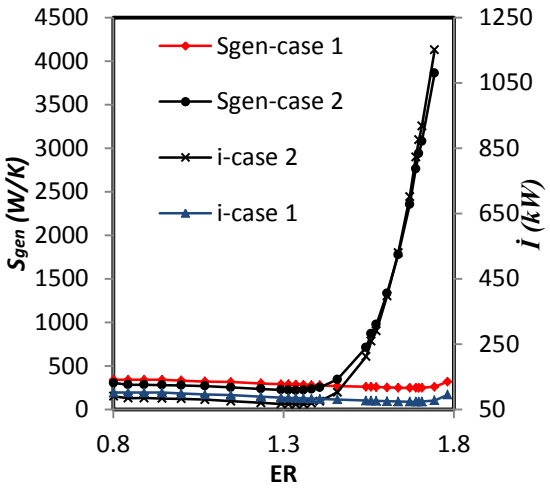

Figure 3 Plots of the variation of entropy generation rate and irreversibilities with ER for case 1 and case 2

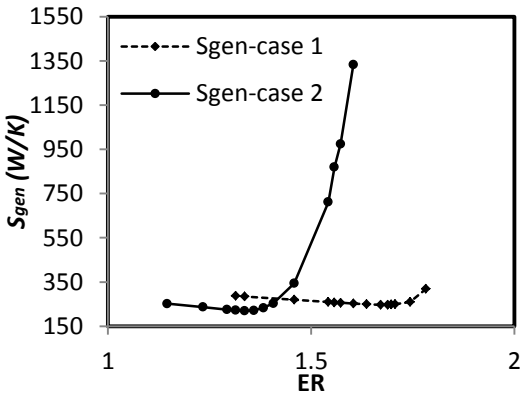

Figure 4 Close up plots of the variation of entropy generation rate with ER for case 1 and case 2

The reason for the deterioration in performance for case 2 could be that the amount of unburnt solid fuel as represented by char, C<s>, has considerably gone up with change in wall condition from adiabatic to negative heat flux as is seen when comparing Figure 5 and Figure 6. The molar fraction of CO did not rise as high for case 2 as was for case 1 as can be seen from Figure 5 and Figure 6.

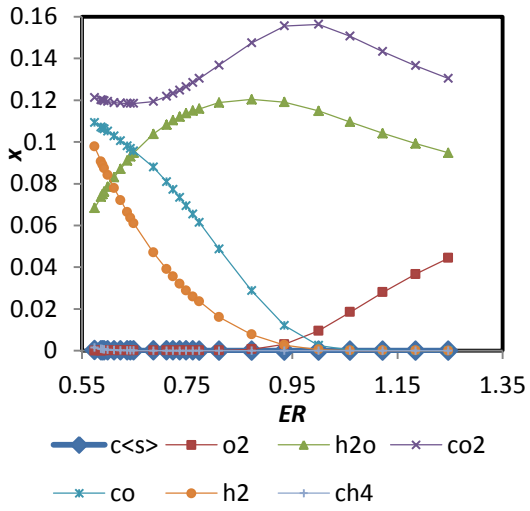

Figure 5 Plot of variation with ER in molar fraction of combustion product species for case 1

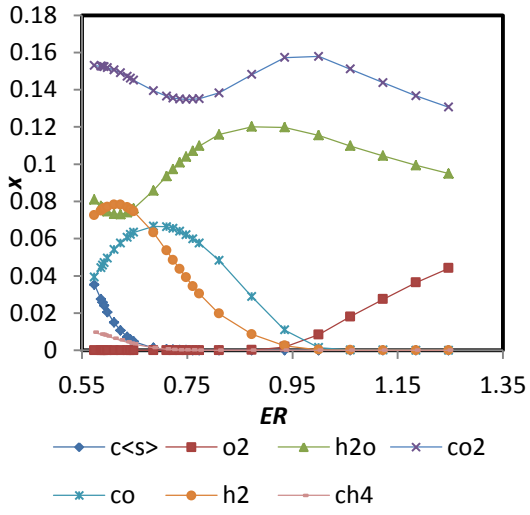

Figure 6 Plot of variation with ER in molar fraction of combustion product species for case 2

As was discussed in [9] and also from observing Figure 5 and Figure 6, the minima entropy generation rates occurred around ER where molar fractions of H_2O and H_2 are equal. This was also the point at which the molar fraction of CO_2 was the lowest. However, Figure 5 and Figure 6 show that the minimum entropy generation rate occurred only at an ER when the molar fraction CO_2 is the lowest, and not when the molar fractions of H_2 and H_2O are equal. Figure 6 also shows that the molar fractions of H_2 and H_2O are equal at two points, which was not observed before with case 1 when the wall condition was adiabatic. Figure 7 shows a plot, with a bound range in the ER axis, of the molar fraction plots of H_2, H_2O and CO_2 for case 1 and case 2, highlighting the difference in response of the combustion products mixture components to a change in wall condition from adiabatic to negative heat flux.

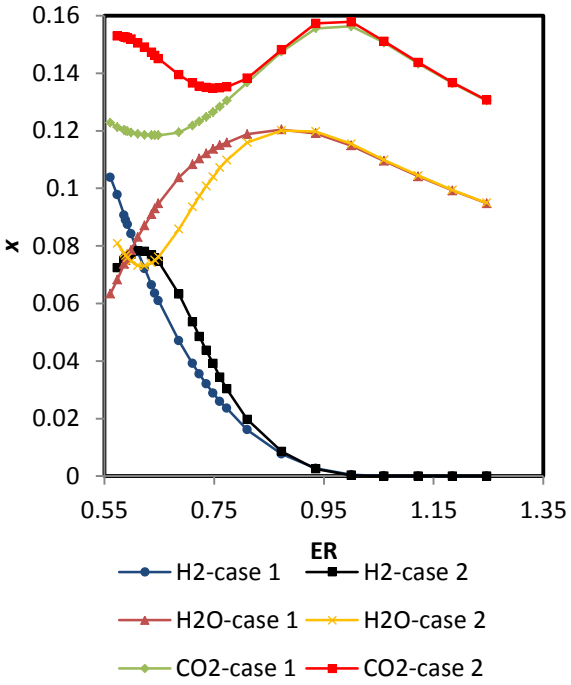

Figure 7 Plot comparing the variation of molar fractions of selected combustion product species with ER for case 1 and case 2

When the wall condition was changed from adiabatic to negative heat flux the penalty paid for deviating from the ER with minimum entropy generation rate was increased drastically, as shown in Figure 8. This was illustrated for example for the case of ER = 1.74 where for case 2 with a negative heat flux wall condition, N_s = 17.62 (i.e. 1662% more $\dot{S}_{gen}$ than $\dot{S}_{gen,\min}$), whereas for the case 1 with an adiabatic wall condition N_s = 1.05 (i.e. 5% more $\dot{S}_{gen}$ than $\dot{S}_{gen,\min}$). At the same ER = 1.74 the corresponding N_R for the case 2 with a negative heat flux wall condition was 13.96 (1296% more $\dot{S}_{gen}$ than $\dot{S}_{gen,th}$), whereas for the case 1 with an adiabatic wall condition N_R = 0.78 (22% less $\dot{S}_{gen}$ than $\dot{S}_{gen,th}$).

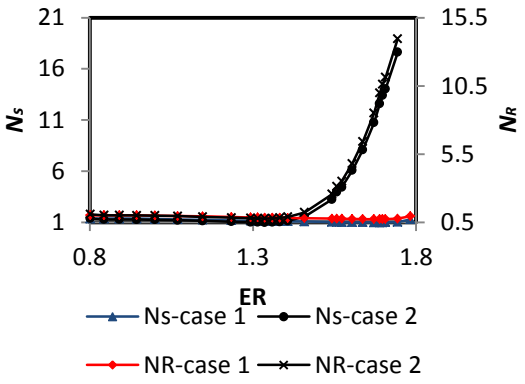

Figure 8 Plot of entropy generation number and relative entropy generation rate as a function of ER for case 1 and case 2

Changing the wall condition from adiabatic to negative heat flux has the effect of lowering the combustor's outlet mixture temperature as shown in Figure 9. As mentioned earlier this is due to the presence of unburnt fuel at the exit in form of char (C<s>).

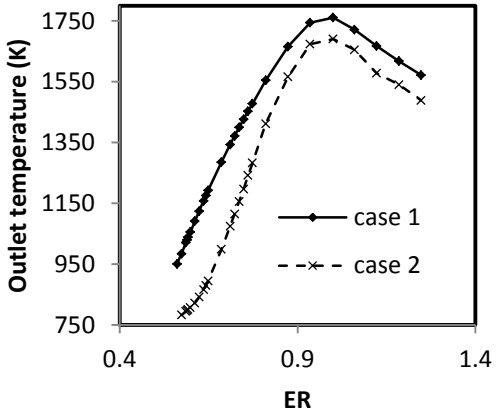

Figure 9 Plot of combustion products mixture temperature as a function of ER for case 1 and case 2

Conclusion

The changing of the wall condition from adiabatic to a negative heat flux resulted in a change in ER, at which minimum entropy generation rate occurred, from 1.67 to 1.34. This also meant that the penalty paid when deviating from that point increased drastically to 1662% for case 2 with a negative heat flux wall condition of 7 500 W/m^2 from 5% for case 1 with an adiabatic wall condition when the combustor is ran at an ER of 1.74.

Acknowledgements

The authors would like express their appreciation to the National Research Foundation (NRF), University of Pretoria and the Council for Scientific and Industrial Research (CSIR) for the financial support and making their infrastructures available for this study.

References

[1] Norton D.G., Vlachos D.G., Combustion characteristics and flame stability at the microscale: a CFD study of premixed methane/air mixtures. Chemical Engineering science 2003; 58: 4871-4882.

[2] Zhang J, Liu P, Zhou Z, Ma L, Li Z, Ni W., A mixed-integer nonlinear programming approach to the optimal design of heat network in a polygeneration energy ststem. Applied Energy 2014; 114: 146-154.

[3] Kohl T, Teles M, Melin K, Laukkanen T, Jarvinen M, Park S.W., Guidici R., Exergoeconomic assessment of CHP-intergrated biomass upgrading. Applied energy 2015; 156: 290-305.

[4] Li S., Jin H., Gao L, Zhang X., Exergy analysis and the energy saving mechanism for coal to synthetic/substitute natural gas and power cogeneration system without and with CO_2 capture. Applied energy 2014; 130: 552-561.

[5] Safari M., Reza M., Sheikhi H., Large eddy simulation-based analysis of entropy generation in a turbulent nonpremixed flame. Energy 2014; 78: 451-457.

[6] Nguyen T., Fulop T.G., Breuhaus P., Elmegaard B., Life performance of oil and gas platforms: Site intergration and themodynamic evaluation. Energy 2014; 73: 282-301.

[7] Hagi H., Le Moullec Y., Nemer M., Bouallou C., Performance assessment of first generation oxy-coal power plants through an exergy-based process integration methodology. Energy 2014; 69: 272-284.

[8] Li C., Gillum C., Toupin K., Donaldson B., Biomass boiler energy conversion system analysis with the aid of exergy-based methods. Energy Conversion and Management 2015; 103: 665-673.

[9] Baloyi J., Bello-Ochende T., Meyer J.P., Thermodynamic optimisation and computational analysis of irreversibilites in a small-scale wood-fired circulating fluidised bed adiabatic combustor. Energy 2014; 70: 653-663.

[10] Le roux W.G., Bello-Ochende T., Meyer J.P., Optimum performance of a small-scale open and direct solar thermal Brayton cycle at various environmental conditions and constraints. Energy 2012; 46 (1): 42-50.

[11] Mwesigye A., Bello-Ochende T., Meyer J.P., Numerical investigation of entropy generation in a

parabolic through receiver at different concentration ratios. Energy 2013; 53: 114-127.
[12] Le Roux W.G., Bello-Ochende T., Meyer J.P., Operating conditions of an open and direct solar thermal Bryaton cycle with optimised cavity receiver and recuperator. Energy 2011; 36 (10): 6027-6-36.
[13] Baloyi J., Bello-Ochende T., Meyer J.P., "The analysis of exergy destruction of a wood fired adiabatic combustor". International Conference on Applied Energy. Pretoria, South Africa, 2013.
[14] Anamalai K., Puri K., Advanced thermodynamics engineering. CRC Press Inc.: Florida, 2002.
[15] Bejan A., Entropy generation minimization: The method of thermodynamic optimization of finite-size systems and finite-time processes. CRC Press Inc.: Florida, 1996.
[16] Kunii D., Levenspiel O., Fluidization Engineering. Stoneham: Massachusetts, 1991.
[17] White F.M., Viscous Fluid Flow. 3rd Ed., International Edition. McGraw-Hill: Singapore, 2006.
[18] ANSYS FLUENT Release 16.2. Theory Guide. ANSYS Inc.: Southpointe, 2011.
[19] Tillman D.A., Rossi A.J., Kitto W.D., Wood Combustion: Principles, Processes and Economics. Academic Press Inc.: New York, 1981.